Effects of ocean acidification and warming on the calcification rate, survival, extrapallial fluid chemistry, and respiration of the Atlantic sea scallop *Placopecten magellanicus*

Running title: Global change effects on sea scallop physiology

Authors: Cameron, L. P.[1*], Grabowski, J. H. [1] and Ries, J. B. [1*]

Cameron, L. P.[1]* cameron.lo@northeastern.edu, ORCID: 0000-0002-6839-2720

Grabowski, J. H.[1] j.grabowski@northeastern.edu

Ries, J. B.[1*], j.ries@northeastern.edu, ORCID: 0000-0001-8427-206X

[1]Department of Marine and Environmental Sciences, Northeastern University Marine Science Center, 430 Nahant Road, Nahant, MA, 01908

*Corresponding authors:

Louise P. Cameron

Cameron.lo@northeastern.edu

Justin B. Ries

j.ries@northeastern.edu

Key words:

Ocean acidification; climate change; multi-stressor; extrapallial fluid; Atlantic sea scallop; *Placopecten magellanicus*; calcification; respiration; mortality

Statement of significance

This manuscript describes the effects of ocean acidification (OA) and warming on the commercially important Atlantic sea scallop. We show that survival, calcification rate, and respiration are sensitive to OA, and that warming affects both survival and calcification. We show that scallops regulate pH and elevate DIC of the extrapallial fluid (EPF) to increase calcification site [CO_3^{2-}], but that regulation of EPF chemistry is insufficient to offset the deleterious effects of OA. This study is the first to characterize the full carbonate system of bivalve EPF under combined OA and warming and provides critical insight into the physiological mechanisms that underlie the response of scallops to global change. Our results highlight the importance of considering the effects of multiple global change stressors on the performance of marine organisms and show that measuring multiple aspects of bivalve physiology can improve our understanding of the mechanisms that drive resilience and sensitivity to global change.

These results should appeal to a broad range of scientists that are interested in the effects of global change on marine organisms. Limnology and Oceanography publishes articles that increase the understanding of aquatic systems, and is widely read by ecologists, biologists, oceanographers, and geologists. We believe that Limnology and Oceanography is the best fit for our paper because it describes novel, hypothesis-driven research that is highly relevant to these audiences.

Abstract

Anthropogenic CO_2-emission is causing ocean warming and acidification. Understanding how basic physiological processes of marine organisms respond to these multiple stressors is important for predicting their responses to future global change. We examined the effects of ocean acidification (OA) and warming (pCO_2 = 344 – 2199 ppm; temperature = 6, 9, 12 °C) on the calcification rate, extrapallial fluid (EPF) carbonate chemistry, respiration, and survivorship of adult Atlantic sea scallops (*Placopecten magellanicus*) in a fully-crossed 143-day experiment. Rates of calcification and respiration were inhibited by OA, and mortality occurred when low calcite saturation state ($\Omega_{calcite}$) was accompanied by high-temperature stress. Declines in growth and, ultimately, survivorship were likely caused by a combination of external shell dissolution, thermal stress, and hypercapnic reduction of metabolic activity under OA. Concentrations of EPF dissolved inorganic carbon (DIC) and total alkalinity (TA) increased above the surrounding seawater concentrations in response to OA. EPF pH declined, but did not decline as much as seawater pH, indicating that scallops regulate EPF pH in support of calcification. The combination of EPF pH regulation and DIC elevation yielded an increase in EPF [CO_3^{2-}] under OA treatments. The combination of low respiration rates, high EPF [CO_3^{2-}], and low calcification rates under OA suggests that the impaired calcification arises more from hypercapnic inhibition of metabolic activity and external shell dissolution than from chemically unfavorable conditions in the EPF. These results demonstrate the importance of EPF chemistry for bivalve biomineralization, but show that regulation efforts are insufficient to fully offset the deleterious effects of OA on scallop performance.

Introduction

Anthropogenic climate change has been described as one of the greatest challenges facing humans today (Dow and Downing 2007). In marine systems, climate warming is accompanied by ocean acidification (OA), which occurs when atmospheric CO_2 equilibrates with the surface ocean and subsequently decreases seawater pH and calcium carbonate saturation state (Doney et al. 2009). Low pH can inhibit glycolytic enzymes (Brooks and Storey 1997; Lannig et al. 2010), impair protein function (De Wit et al. 2018), and cause homeostatic imbalance and tissue acidosis in marine organisms (Pörtner et al. 1998; Michaelidis et al. 2005). Many marine organisms build protective structures from calcium and carbonate ions (Lowenstam and Weiner 1989), and a decline in calcium carbonate saturation state therefore makes calcification more challenging due to decreased substrate availability for calcification. Predicting the effects of global change is complex, as OA and temperature change are occurring simultaneously, and may occur at different rates and in different directions within and among marine systems (Gunderson et al. 2016). Ocean acidification and warming cause organismal stress through multiple pathways including reductions in calcification, survival, and reproductive fitness (Kroeker et al. 2013). Thus, an in-depth understanding of the responses to global change at scales ranging from the biochemical to the whole organism is required to identify patterns of vulnerability and resilience across species. Understanding how these stressors affect the uptake of energy by organisms, and how this energy is then allocated for different biological processes, provides a framework for exploring threshold responses to OA and warming for marine organisms.

The majority of OA research to date addresses effects on biological calcification. Although many marine organisms exhibit reduced calcification in response to OA (Gazeau et al. 2007; Ries et al. 2009; Brennand et al. 2010; Reymond et al. 2012), some do not respond (Ries et al. 2009; Rodolfo-Metalpa et al. 2011), and others increase their calcification rates under OA

scenarios (Wood et al. 2008; Ries et al. 2009). Observations of elevated pH at the site of calcification across calcifying taxa (de Nooijer et al. 2009; Ries 2011; McCulloch et al. 2012; Sutton et al. 2018; Liu et al. 2020) are consistent with the assertion that some marine calcifiers can mitigate the effects of CO_2-induced OA by modifying calcifying fluid chemistry in a manner that supports calcification and/or reduces shell dissolution. One strategy is to increase pH at the site of calcification, which permits utilization of the increased seawater DIC by converting it to carbonate ions for calcification. This mechanism may be driven by the exchange of hydrogen and calcium ions at the site of calcification by ATPase proton pumps (Al-Horani et al. 2003; Zoccola et al. 2004). Although the energetic cost of maintaining calcification site pH has yet to be measured, increasing the activity of ion channels and ATPases should require energy, potentially diverting energy from other physiological processes such as reproduction (Morita et al. 2010) and tissue maintenance (Wood et al. 2008).

It is important to consider the effects of different combinations of OA and warming on the physiology of marine organisms due to their potential for interaction. Organisms exist within 'windows' of thermal tolerance, where respiration is maximal at an optimal temperature and lower at either side of that temperature (Pörtner and Farrell 2008). Ocean acidification can narrow this thermal window (Pörtner 2008) and limit oxygen uptake in some bivalve species (Michaelidis et al. 2005), although . the effects of warming and acidification are highly dependent on the species and physiological performance metrics studied (Lefevre 2016). In some species, warming has been shown to exacerbate the negative effects of OA on calcification in some species due to additive physiological stress (Talmage and Gobler 2011). In other species, warming can mitigate the negative effects of OA on calcification (Kroeker et al. 2014; Harney et al. 2016) by reducing CO_2 solubility (Millero 2007), or by stimulating metabolism in support of

110 calcification (Gillooly et al. 2001). Warming and acidification may also have additive (Crain et
111 al. 2008) or synergistic (Parker et al. 2010; Rodolfo-Metalpa et al. 2011) effects on physiology.
112 In the Pacific oyster, warming caused stress responses while simultaneously alleviating the
113 negative effects of acidification on calcification (Ko et al. 2014).

114 Bivalve shell mineralization occurs in the extrapallial fluid (EPF), which occupies a
115 semi-enclosed space between the outer mantle epithelium and innermost shell (Crenshaw and
116 Neff 1969). This fluid contains the raw materials needed for calcification, such as calcium and
117 carbonate ions (Crenshaw 1972), ion binding proteins (Misogianes and Chasteen, 1979; Hattan et
118 al. 2000; Ma et al. 2007), silk fibroin proteins (Addadi et al. 2006), and chitin (Addadi et al.
119 2006). Nacre formation is disrupted when the EPF is removed, and EPF proteins affect crystal
120 growth *in vitro*, suggesting that it plays an important role in bivalve calcification (Wilbur and
121 Bernhardt, 1983; Xie et al. 2016). Bivalve EPF pH is typically lower than seawater pH
122 (Crenshaw and Neff 1969; Crenshaw 1972; Downey-Wall et al. 2020), and bivalves are
123 particularly sensitive to OA (Gazeau et al. 2013; Ries et al. 2009; Waldbusser et al. 2015;
124 Thomsen et al. 2015). This suggests that bivalves cannot mitigate the effects of OA on
125 calcification simply through EPF pH regulation.

126 The Atlantic sea scallop (*Placopecten magellanicus*) supports one of the most
127 profitable fisheries in the United States (Hart and Rago 2011). Their habitat in the Northwest
128 Atlantic is experiencing high rates of warming (Pershing et al. 2015), and acidification (Bates et
129 al. 2012), but there have been no studies to date on this species' response to OA. Studies of other
130 pectiniids have revealed mixed responses to OA. The bay scallop *Argopecten irradians* exhibited
131 reduced calcification under OA (Ries et al. 2009; White et al. 2013), whereas the calcification
132 rate of the king scallop *Pecten maximus* appears relatively resilient to OA (Sanders et al. 2013;

Cameron et al. 2019). Here, we examine the independent and interactive effects of OA and warming on the calcification rate, EPF chemistry (pH, DIC, TA and $[CO_3^{2-}]$), respiration, and survivorship of adult Atlantic sea scallops (*Placopecten magellanicus*) in a fully-crossed 143-day pCO_2 (present-day: 400 ppm, year 2100: 800 ppm, year 2300: 2050 ppm) and temperature (6, 9, 12 °C) experiment.

Methods

Collection of scallops from Georges Bank

Scallops were collected from 3 regions of Georges Bank known to contain high scallop density (Stokesbury et al. 2004). Nine tows, spanning a range of depths and locations on Georges Bank (Table S1.1), were each conducted for 15 minutes at 3.8 knots (7 km/h) with a single New Bedford-style dredge lined with a 2.54 cm mesh which retained small scallops. The physical and chemical conditions at each collection site are summarized in Table S1.2. Scallops obtained from the tows were stored alive in buckets refreshed with flow-through seawater on the deck and used in the tank experiment described below.

Design of controlled laboratory experiment

Prior to assignment to treatment tanks, scallops (shell height = 75.25 mm ± 2.18 (mean ± SE)) were acclimated to laboratory conditions in three 2400-litre (1.83 m diameter x 1.22 m deep) holding tanks with flow-through natural seawater that was refreshed at a rate of 5-10 L/min for two weeks. Water was supplied from an offshore pipe located near Pumphouse Beach, Nahant. Scallops that died during transport or that exhibited signs of morbidity (e.g., gaping shells, weak clap strength) during this period were removed, yielding a total of 142 scallops from field sites

C-E (S1). Scallops from different field sites were spread evenly across 42-L replicate tanks (n = 3) at each treatment level (Table S1.3). This resulted in tanks containing either 5 or 6 individuals (Table S1.4). The experiment was conducted using an orthogonal design that included three temperature regimes crossed with three pCO_2 regimes (Table S2).

Scallops were introduced to tanks bubbled with compressed ambient air at a temperature of 9 °C. Experimental tanks were connected to a flow-through system that refreshed the tank water at a rate of 150 mL/min. Scallops were acclimated to these initial conditions for one week, after which conditions were gradually adjusted to target conditions over a two-week period. The temperature treatments used in this experiment were 6, 9, and 12 °C. Scallops currently experience this temperature range on Georges Bank, but do not typically experience 12 °C for extended periods of time (Butnam and Beardsley 1987). The long exposure to 12 °C is therefore reflective of temperature conditions that sea scallops will likely experience under predicted future warming (IPCC 2019; Pershing et al. 2015). The pCO_2 treatments of 400, 800, and 2050 ppm were chosen to reflect present-day open ocean (control), predicted end of 21st century (moderate-increase), and predicted end of 23rd century (high-increase) values (IPCC 2019). During the acclimation phase of the experiment, temperature was adjusted by 0.5 °C every second day in the high and low temperature tanks. Air and pCO_2 mass flow controllers (described in detail below) were adjusted daily to increase seawater pCO_2 by 100 ppm per day in year 2100 scenario tanks and by 280 ppm per day in year 2300 tanks, until target treatments were reached. Once target treatments were reached, the specimens were acclimated for an additional 18-days before any physiological measurements were obtained. Scallops were then exposed to experimental conditions for 143 days, during which the following physiological measurements were obtained: calcification rates (measured over the first 85 days), respiration rates (measured

between days 77 and 83), and EPF chemistry (measured between days 136 and 143). Scallops were batch fed daily with 1% Reed Mariculture Shellfish Diet ™ throughout the experiment. Food volume was calculated according to the maximum tank biomass across all replicate tanks (Helm and Bourne, 2004). Filtration systems were bypassed for one hour during feeding.

Measurement and control of the experimental seawater carbonate system

The temperature of all experimental tanks was controlled to within 0.1 °C using Aqua Euro USA model MC-1/4HP chillers. The carbonate chemistry of tanks was controlled using a combination of air and CO_2 solenoid-valve mass flow controllers (Aalborg, Model GFC17, precision = 0.1mL/min). For control pCO_2 treatments, compressed CO_2-free air was produced with a Parker Balston FT-IR Purge Gas Generator and then mixed with compressed CO_2 at flow rates proportional to target pCO_2 conditions. For all elevated pCO_2 conditions, compressed ambient air was mixed with compressed CO_2 to produce the target pCO_2 condition.

Temperature, pH, and salinity of all replicate tanks were measured three times per week for the duration of the experiment. Seawater pH was measured using an Accumet solid state pH electrode (precision = 1mV), salinity with a YSI 3200 conductivity probe (precision = 0.1), and temperature with a glass thermometer (precision = 0.05 °C). Every two weeks, seawater samples were collected from each replicate tank for analysis of dissolved inorganic carbon (DIC) and total alkalinity (TA). Samples were collected in 250 mL borosilicate glass bottles sealed with a vacuum-greased ground-glass stopper and immediately poisoned with 100 µL saturated mercuric chloride ($HgCl_2$) solution. Samples were refrigerated and analyzed for TA via closed-cell potentiometric Gran titration and for DIC with a UIC coulometer within a VINDTA 3C system (Marianda Corp.). Seawater DIC, TA, salinity, pressure, and temperature were used to calculate $\Omega_{calcite}$, pH, $[CO_3^{2-}]$, $[HCO_3^-]$, $[CO_2]$, and pCO_2 of each sample using CO_2SYS version 2.1, using

the seawater pH scale with K_1 and K_2 values from Roy et al. (1993), a $KHSO_4$ value from Dickson (1990), and a $[B]_T$ value from Lee et al. (2010). Calcite saturation state ($\Omega_{calcite}$) is presented because the scallop prodissoconch is primarily calcite (Krantz et al. 1984).

Performance measurements

Calcification rates were measured over the first 85 days of the experiment by buoyantly weighing all scallops at the start of the experiment, and again after 85 days (Section S3 in Supporting Information). At the end of the experimental period, scallops were shucked and shells were soaked in 100% ethanol to remove seawater and any superficially precipitated salts. Shells were then dried, and the dry shell weight was regressed against final buoyant weight measurement to establish an empirical relationship between the buoyant and dry shell weights (Figure S3.1):

$$\text{Dry weight (g)} = 1.596 \times \text{buoyant weight} - 0.222$$

This empirical relationship was then used to calculate dry shell weight at each buoyant weight time point (Ries et al. 2009). Net calcification rates were calculated as the percentage weight-change between the initial and final dry shell weights.

Respiration rates were measured on 3 individuals per replicate tank during the 11^{th} week (days 77 – 83) of the experiment. Each respiration trial took a total of 120 minutes (30 minutes of acclimation and 90 minutes of respiration measurements). Scallops were placed in sealed respiration containers (height = 70 mm, diameter = 130 mm, volume = 1100 mL) filled with seawater equilibrated at the treatment pCO_2 and temperature conditions. A PreSens SP-PSt-NAU oxygen sensor dot (accuracy = ± 0.1 % O_2 at 20.9 % O_2; drift < 0.03 % O_2 within 30 days) was glued to the inside of the lid of each container to record oxygen concentration during respiration measurements. Sensors were calibrated as described in the PreSens manual via a 2-point

calibration with N_2 gas and air. Respiration rate was reported as oxygen consumption per hour normalized to dry tissue weight (g) (Section S4 in Supporting Information).

In the 12th week of the experiment (days 91 – 94), ports (derived from modified plastic pipette tips) for extracting and measuring EPF were inserted into the shells of all scallops following the method described in Stemmer et al. (2019). Three 3-mm holes were drilled into the right valve of each scallop along the central band perpendicular to the umbo. Holes were spaced evenly, with one hole placed approximately ⅓ of the shell height from the umbo, one approximately ⅓ of the shell height from the pallial line, and one drilled at an even spacing between the other two. This design was intended to maximize the volume of EPF extracted, as membranes may divide the extrapallial space of bivalves into multiple compartments (Stemmer et al. 2019). Drill sites were flushed with seawater during drilling to minimize frictional heating. A pipette tip, cut to a length of 5 mm, was then sealed into place in each hole using marine-safe cyanoacrylate (Starbond EM-2000 CA USA) so that the narrowest end was flush with the drilled hole, and then sealed with parafilm to prevent mixing of the EPF with seawater. This served as a port to allow extraction of EPF via syringe. Following this procedure, scallops were returned to their treatment conditions for 45 days before any extractions or measurements of EPF were performed. To extract scallop EPF, scallops were removed from their experimental treatments and patted dry with a paper towel. The parafilm that sealed the port was removed and approximately 0.5 mL of EPF was extracted using a 5 mL syringe fitted with a flexible 18-gauge polypropylene tip. The port was then re-sealed with parafilm and scallops were returned to their treatment tanks. Extrapallial fluid was extracted on days 136 – 143.

Extrapallial fluid pH was immediately measured following extraction with an Orion 91’10DJWP double junction micro-pH probe standardized with pH 7 and 10 NBS buffers.

Extrapallial fluid samples were stored in 2 mL microcentrifuge tubes and refrigerated for subsequent analysis of DIC. DIC was analyzed using an Apollo SciTech AS-C2 dissolved inorganic carbon analyzer calibrated with a Dickson seawater CRM. The salinity of the EPF was measured with a Mettler Toledo InLab Expert Pro-ISM conductivity probe calibrated with a Dickson seawater CRM. Measured pH_{NBS}, DIC, temperature, and salinity were then used to calculate pH on seawater scale (pH_{SW}), [CO_3^{2-}], [HCO_3^-], [CO_2], and pCO_2 of each sample using CO_2SYS version 2.1, using K1 and K2 values from Roy et al. (1993), a $KHSO_4$ value from Dickson (1990), and a $[B]_T$ value from Lee et al. (2010).

To understand the influence of proton regulation on the EPF carbonate system, the

Likewise, a constant

Scallops that died during the experiment were immediately removed from their experimental treatment and their day of death was recorded.

Statistical analysis

Linear mixed effects models were used to investigate the effects of seawater $\Omega_{calcite}$ and temperature on calcification rate, respiration rate, and EPF chemistry (pH, DIC, TA, [CO_3^{2-}],). Replicate tank was modeled as a random effect. Normality of residuals was tested

using a Shapiro-Wilk test, and plots of residuals vs. fitted values were generated to test the assumption of homoscedasticity. All trends were visually inspected using scatterplots to ensure that the data met the assumption of normality. Extrapallial fluid [CO_3^{2-}] was log-transformed to meet the assumption of normality of residuals. The linear mixed effects models used to test the responses of respiration rate to $\Omega_{calcite}$ and temperature did not meet the assumptions of normality of residuals or homoscedasticity. To account for this, linear regression permutation tests were conducted using the aovperm function in the R statistical package 'permuco' (Frossard and Renaud 2019). For these tests, 10,000 iterations were performed using the method for handling nuisance variables described in Kherad-Pajouh (2010). Replicate tank was included as a random effect in permutation models. Linear mixed effects models were also used to test the correlation between respiration rate and calcification rate in each pCO_2 treatment, and to test correlations between calcification rate and EPF pH, DIC, TA and [CO_3^{2-}]. The assumptions of these tests were examined following the protocol described above. A proportional hazards model was used to test the effects of seawater $\Omega_{calcite}$ and temperature on survivorship. This analysis discounted mortality that occurred during EPF extraction, as the stress effect of the drilling and fluid extraction processes are unknown.

A model selection approach was developed to identify the model that best explained the data for each linear mixed effects model. For all tests, models were first generated to test the effects of seawater $\Omega_{calcite}$, temperature, collection site depth, and collection site $\Omega_{calcite}$ on the response variable. The most complex model was run first with interaction terms between these variables. If no interaction terms were significant, this term was dropped and a new model was run excluding this interaction term but including others. This process was repeated until only significant interactions remained. If no interactions were significant, a model was generated

testing the additive effects of these predictors. Predictor terms were dropped if doing so improved the AIC value of the final model. When an interaction between seawater $\Omega_{calcite}$ and temperature was significant, the model output was plotted at each temperature to understand how temperature altered the effect of seawater $\Omega_{calcite}$.

Model outputs were used to estimate thresholds of growth, persistence, and mortality according to various combinations of seawater $\Omega_{calcite}$ and temperature. Sequences of temperature (range = 6 - 12 °C, step size = 0.05) and $\Omega_{calcite}$ (range = 1-3.5, step size = 0.01) were generated and models predicting calcification rate and survivorship were constrained with these values. Combinations of temperature and seawater $\Omega_{calcite}$ that resulted in positive calcification rates and survival rates of greater than 50 % (LD^{50}) were extracted and used to define contours of growth and survivorship. All statistical analyses were conducted with RStudio version 0.99.903.

Results

Respiration rate

Respiration rates of Atlantic sea scallops ranged from 0.03 to 1.21 mg O_2 g^{-1} (of tissue) hr^{-1} and were significantly correlated with seawater $\Omega_{calcite}$ (Fig. 1a; aovperm, $F_{1,69} = 4.958$, $p = 0.029$). Neither temperature (aovperm, $F_{1,69} = 0.133$, $p = 0.875$) nor the interaction between temperature and seawater $\Omega_{calcite}$ (aovperm, $F_{1,69} = 0.258$, $p = 0.771$), significantly affected respiration rate.

311

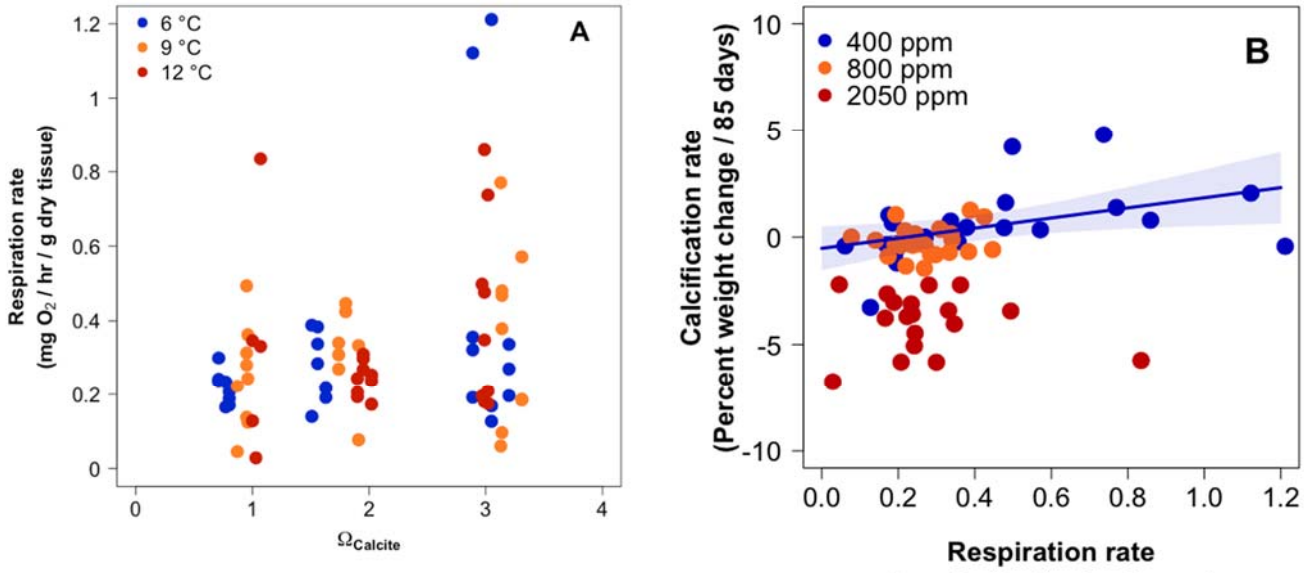

Figure 1. The impact of seawater $\Omega_{calcite}$ and temperature on respiration rate (A) and the relationship between respiration rate and calcification rate (B) of the Atlantic sea scallop *Placopecten magellanicus* after 77 days of exposure to experimental pCO_2 and temperature treatments. Decreasing $\Omega_{calcite}$ resulted in a significant decline in respiration rate (aovperm, $F_{1,69} = 4.958$, $p = 0.029$), while temperature did not significantly influence respiration rate (aovperm, $F_{1,69} = 0.133$, $p = 0.875$). There was a positive correlation between respiration rate and calcification rate in the control pCO_2 treatment (400 ppm, LME, $p = 0.017$, $t_{21} = 2.60$), but not in the moderate (800 ppm, LME, $p = 0.463$, $t_{20} = 0.75$) or high (2050 ppm, LME, $p = 0.686$, $t_{16} = 0.41$) pCO_2 treatments. The solid line represents the trend line generated from linear mixed effects models; shaded region represents the 95% confidence intervals of this trend.

312

313 *Extrapallial fluid chemistry*

314 Extrapallial fluid pH ranged from 6.27 to 7.77 (NBS scale). Treatment means were always lower

315 than seawater pH and there was a strong positive correlation between EPF pH and seawater

316 $\Omega_{calcite}$ (Fig. 2a, Table 2, LME, $p = 0.006$, $t_{39} = 2.90$). On the other hand, both EPF DIC and

317 TAwere typically greater than seawater levels in the year 2100 and 2300 pCO_2 treatments, but

318 were less

than seawater levels under the present-day pCO_2 treatment. Extrapallial fluid DIC ranged from 293 to 30,197 µmol/L, and EPF TA ranged from 314 to 28,298 µmol/L.

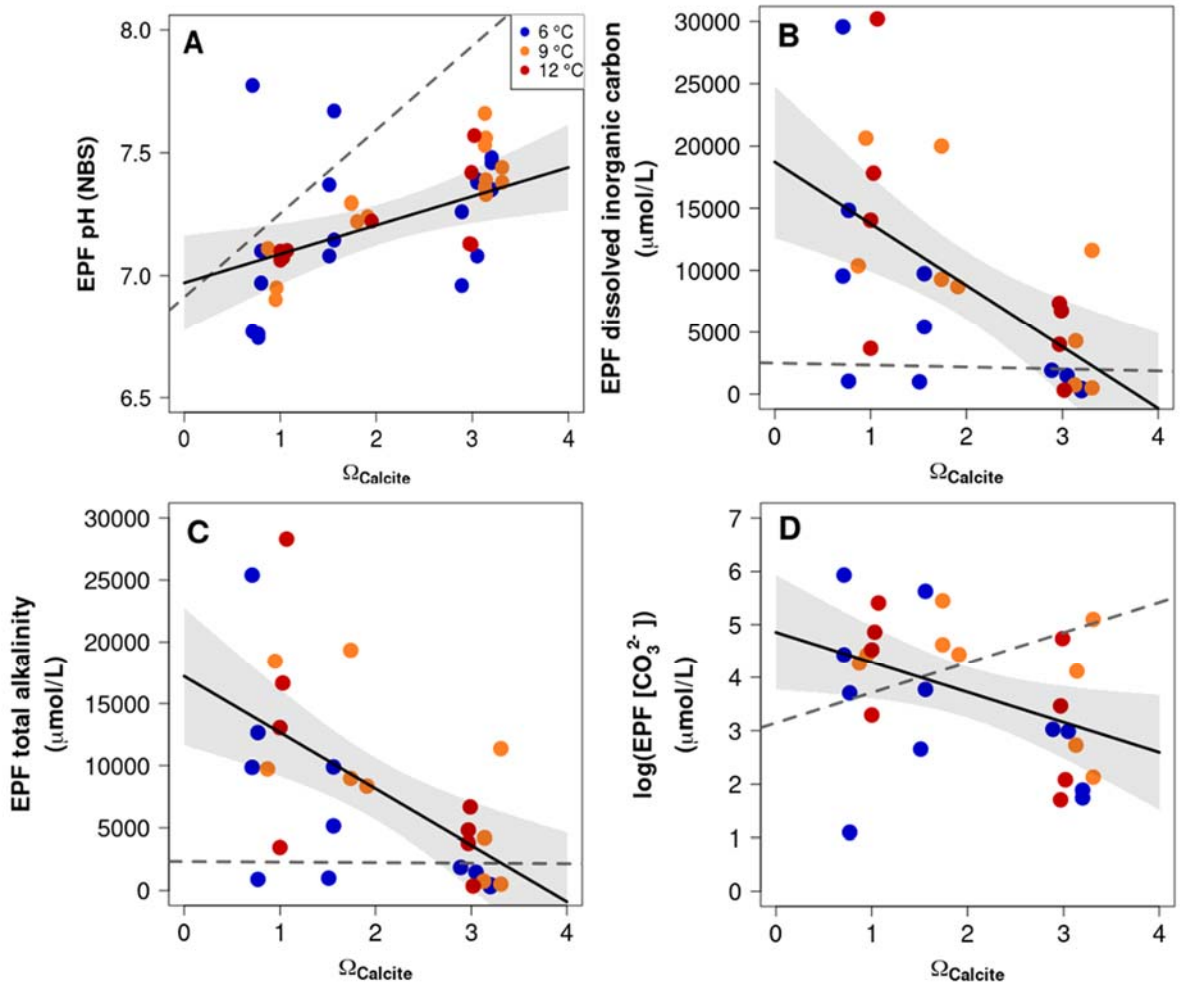

Figure 2. The effect of seawater $\Omega_{calcite}$ and temperature on pH (A), dissolved inorganic carbon (DIC; B), total alkalinity (TA; C), and the log-transformed carbonate ion concentration ($[CO_3^{2-}]$; D) of the Atlantic sea scallop (*Placopecten magellanicus*). The solid lines represent trend lines generated from linear mixed effects models; shaded regions represent the 95% confidence intervals of this trend. Dashed gray lines represent seawater pH (A), DIC (B), TA (C) and CO_3^{2-} (D).

Table 2. Summary of carbonate system parameters of Atlantic sea scallop extrapallial fluid (EPF), extracted on final day of experiment. Average measured EPF parameters: salinity, pH on the NBS scale (pH_{NBS}), and dissolved inorganic carbon (DIC). Average calculated EPF parameters: pCO_2, EPF pH on the seawater scale (pH_{SW}), total alkalinity (TA), carbonate ion concentration ($[CO_3^{2-}]$), bicarbonate ion concentration ($[HCO_3^-]$), dissolved CO_2 ($[CO_2]_{(SW)}$), calcite saturation state ($\Omega_{calcite}$), and Δ-total alkalinity (ΔTA; i.e., EPF TA – SW TA). 'SD' is standard deviation; 'n' is number of observations.

Measured parameters		Control pCO_2			Moderate pCO_2			High pCO_2		
		6 °C	9 °C	12 °C	6 °C	9 °C	12 °C	6 °C	9 °C	12 °C
Sal	**(psu)**	33.4	31.9	33.6	33.7	31.7	33.6	33.6	32.2	33.6
	SD	2.1	0.3	0.7	1.8	0.4	NA	1.2	1.1	1.1
	Range	30.3 - 35.6	31.6 - 32.2	32.9 - 34.6	31.2 - 35.9	31.0 - 32.2	NA	32.2 - 35.1	31.3 - 33.3	32.8 - 35.2
	n	5	5	5	5	6	1	4	3	4
pH_{NBS}		7.30	7.46	7.10	7.30	7.28	7.22	7.02	6.99	7.09
	SD	0.19	0.12	0.50	0.27	0.28	NA	0.40	0.11	0.02
	Range	6.96 - 7.48	7.33 - 7.66	6.27 - 7.57	7.03 - 7.67	6.68 - 7.58	NA	6.75 - 7.77	6.90 - 7.11	7.06 - 7.10
	n	8	8	5	5	6	1	6	3	4
DIC	**(µM)**	1043	4286	4618	5396	12634	NA	13750	15503	16436
	SD	791	5184	3208	4374	6356	NA	11975	7247	10947
	Range	293 - 1919	506 - 11614	332 - 7362	1000 - 9886	8704 - 19995	NA	1046 - 29562	10379 - 20627	3690 - 30197
	n	4	4	4	3	3	0	4	2	4
Calculated parameters										
pCO_2 (gas-e)	**(ppm-v)**	858	3424	18656	3645	13140	NA	33939	32477	29445
	SD	767	4303	29296	3051	5906	NA	39587	23636	18878
	Range	160 - 1837	353 - 9511	187 - 62402	738 - 6822	9456 - 19952	NA	2528 - 85341	15763 - 49190	6424 - 52276
	n	4	4	4	3	3	0	4	2	4
pH_{SW}		7.56	7.60	7.22	7.59	7.42	NA	7.19	7.15	7.19
	SD	0.10	0.08	0.60	0.29	0.03	NA	0.55	0.15	0.02
	Range	7.44 - 7.69	7.54 - 7.70	6.37 - 7.72	7.32 - 7.90	7.39 - 7.45	NA	6.90 - 8.01	7.04 - 7.26	7.17 - 7.21
	n	4	4	4	3	3	0	4	2	4
TA	**(µM)**	1031	4212	3911	5344	12221	NA	12200	14082	15363
	SD	757	5058	2652	4448	6175	NA	10122	6160	10262
	Range	314 - 1861	518 - 11364	359 - 6675	995 - 9886	8345 - 19342	NA	902 - 25390	9727 - 18438	3463 - 28298
	n	4	4	4	3	3	0	4	2	4
$[CO_3^{2-}]$	**(µM)**	13	62	40	112	140	NA	126	78	118
	SD	8	72	51	144	81	NA	170	9	82
	Range	6 - 21	8 - 164	6 - 114	14 - 277	85 - 233	NA	3 - 376	72 - 84	27 - 223
	n	4	4	4	3	3	0	4	2	4
$[HCO_3^-]$	**(µM)**	987	4069	3817	5101	11929	NA	11934	13920	15119
	SD	745	4917	2585	4175	6013	NA	10118	6144	10098
	Range	158 - 1820	482 - 11020	317 - 6427	950 - 9299	8165 - 18863	NA	892 - 25218	9575 - 18265	3400 - 27842
	n	4	4	4	3	3	0	4	2	4
$[CO_2]$	**(µM)**	43	155	762	183	595	NA	1690	1505	1199
	SD	38	195	1197	153	264	NA	1975	1093	769
	Range	8 - 92	8 - 164	8 - 2550	37 - 341	85 - 233	NA	125 - 4260	732 - 2278	262 - 2132
	n	4	4	4	3	3	0	4	2	4
$\Omega_{CALCITE}$		0.32	1.51	0.96	2.71	3.38	NA	3.03	1.90	2.83
	SD	0.19	1.74	1.22	3.52	1.94	NA	4.09	0.21	1.97
	Range	0.14 - 0.49	0.20 - 3.97	0.13 - 2.74	0.34 - 6.76	2.05 - 5.60	NA	0.07 - 9.04	1.75 - 2.05	0.65 - 5.37
	n	4	4	4	3	3	0	4	2	4
ΔTA		-1197	2009	1737	3115	9954	NA	9852	11742	13062
	SD	758.00	5058	2651	4443	6177	NA	10124	6162	10259
	Range	-1915 - -367	-1685 - 9161	-1817 - 4496	-1227 - 7653	6076 - 17077	NA	-1450 - 23046	7385 - 16099	1164 - 25993
	n	4	4	4	3	3	0	4	2	4

Extrapallial fluid DIC (Fig. 2b, LME, $p = 0.001$, $t_{24} = -3.74$), TA (Fig. 2c, LME, $p = 0.001$, $t_{24} = -3.75$), and $[CO_3^{2-}]$ (Fig. 2d, log-transformed $[CO_3^{2-}]$; LME, $p = 0.025$, $t_{24} = -2.40$)

were all significantly negatively correlated with seawater $\Omega_{calcite}$—meaning that these critical carbonate system parameters of the EPF became more supportive of calcification under acidified conditions. Temperature did not significantly affect any aspect of the EPF carbonate system (LMEs, pH: $p = 0.549$, $t_{39} = -0.61$; DIC: $p = 0.351$, $t_{24} = 0.95$; TA, $p = 0.343$, $t_{24} = 0.97$; $[CO_3^{2-}]$: $p = 0.466$, $t_{24} = 0.74$).

Both (Fig. S5b, LME, $p = 0.001$, $t_{24} = -3.71$) $\Omega_{calcite}$ declined. Assuming that seawater TA represents the starting conditions of the EPF prior to manipulation by the scallop (i.e., the ultimate source of the EPF is seawater), increasing $\Omega_{calcite}$ indicates that more protons were being removed from the EPF in the lower $\Omega_{calcite}$ (i.e., acidified) treatments, apparently to increase EPF $[CO_3^{2-}]$ in support of calcification—potentially at an increased energetic cost.

Environmental influences on calcification rate

Calcification rates of Atlantic sea scallops were significantly affected by the interaction of seawater $\Omega_{calcite}$ and temperature (LME, $F_{1,129} = 21.491$, $p<0.001$). Under all temperatures, calcification rate declined with decreasing $\Omega_{calcite}$, with the slope of this decline increasing with increasing temperature (Fig. 3).

Physiological influences on calcification rate

There was a significant correlation between respiration rate and calcification rate under present-day pCO_2 (Fig. 1b, LME, $p = 0.017$, $t_{21} = 2.60$), although this relationship was not found in either the year 2100 (LME, $p = 0.463$, $t_{20} = 0.75$) or year 2300 (LME, $p = 0.686$, $t_{16} = 0.41$) pCO_2

347

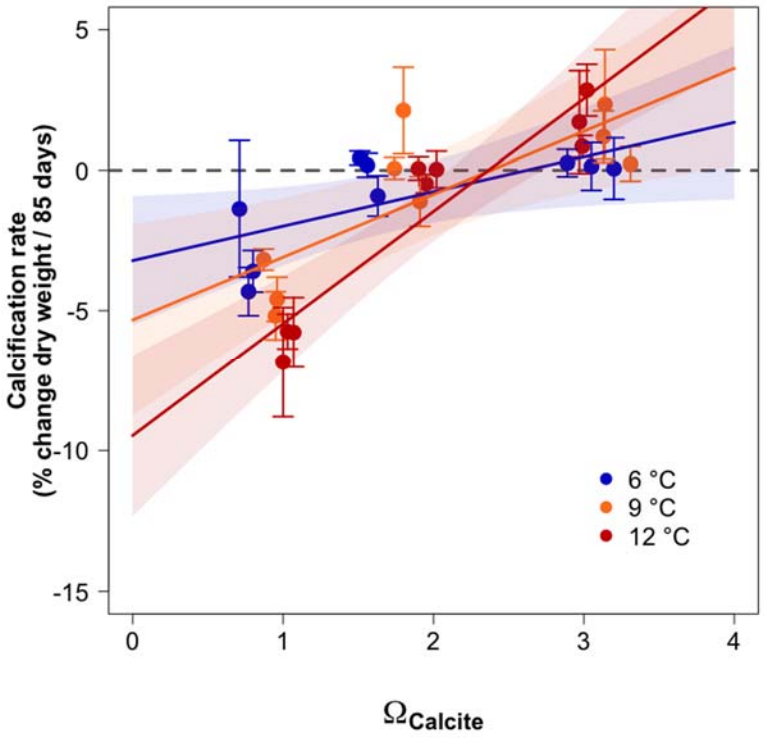

Figure 3. The impact of seawater $\Omega_{calcite}$ and temperature on the calcification rate (%-change in dry weight) of the Atlantic sea scallop *Placopecten magellanicus* over 143-day experiment. The solid lines represent trend lines generated from linear mixed effects models; shaded regions represent the 95% confidence intervals of this trend. The dashed line defines the boundary between net calcification (above line) and net dissolution (below line). Closed circles represent treatment tank means and error bars represent standard error of mean amongst replicate tanks.

348

349 treatments. Calcification rate was also significantly affected by the three-way interaction
350 between EPF pH, temperature, and seawater $\Omega_{calcite}$ (LME, $F_{1,21} = 5.530$, $p = 0.029$). At 6 °C, the
351 calcification rate was significantly positively correlated with both EPF pH and seawater $\Omega_{calcite}$
352 (Fig 4, LME, EPF pH, $p = 0.009$, $t_{12} = 3.14$; seawater $\Omega_{calcite}$, $p = 0.018$, $t_{12} = 2.75$). At 9 °C,
353 there was no significant correlation between EPF pH and calcification rate (Fig. 4, LME, $p =$
354 0.129, $t_7 = 1.72$). At 12 °C, there were not enough surviving individuals to confidently evaluate
355 whether a correlation existed between EPF pH and calcification rate (Fig. 4, N = 3).

356

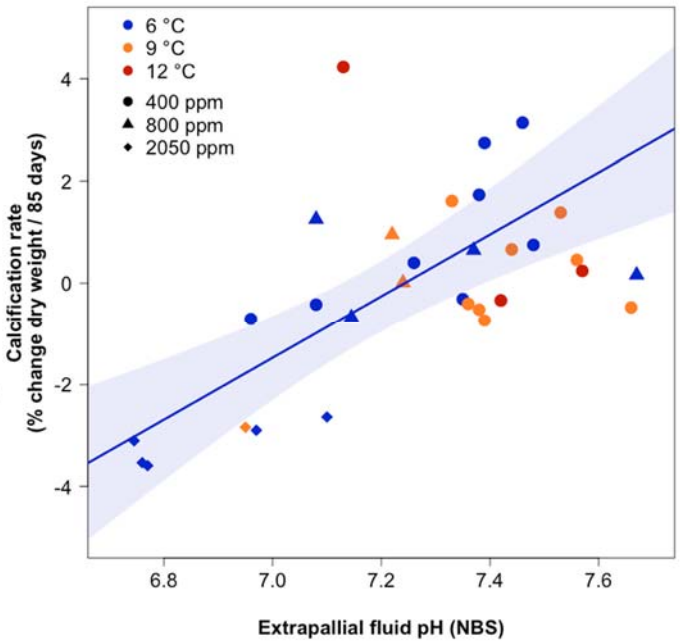

Figure. 4 The relationship between scallop calcification rate and EPF pH at 6, 9, and 12 °C. The significant linear relationship between extrapallial fluid pH and calcification rate at 6 °C is indicated by the solid blue line, and the shaded region represents the 95% confidence interval of the regression.

357 *Survivorship*

358 There was a statistically significant effect of both seawater temperature and $\Omega_{calcite}$ on
359 survivorship (Fig. 5; proportional hazards model; temperature, $p < 0.001$, $z = 4.39$; $\Omega_{calcite}$, $p =$
360 0.036, $z = -2.10$), with increased temperature and OA having an additive, negative effect on
361 survivorship. Lethal dose thresholds at 50 % (LD_{50}) mortality were not reached at any
362 temperature under the present-day pCO_2 treatment, but were reached at 11.4 – 11.9 °C under the
363 year 2100 pCO_2 treatment, and at 10.4 – 10.7 °C under the year 2300 pCO_2 treatment (Fig. 6).

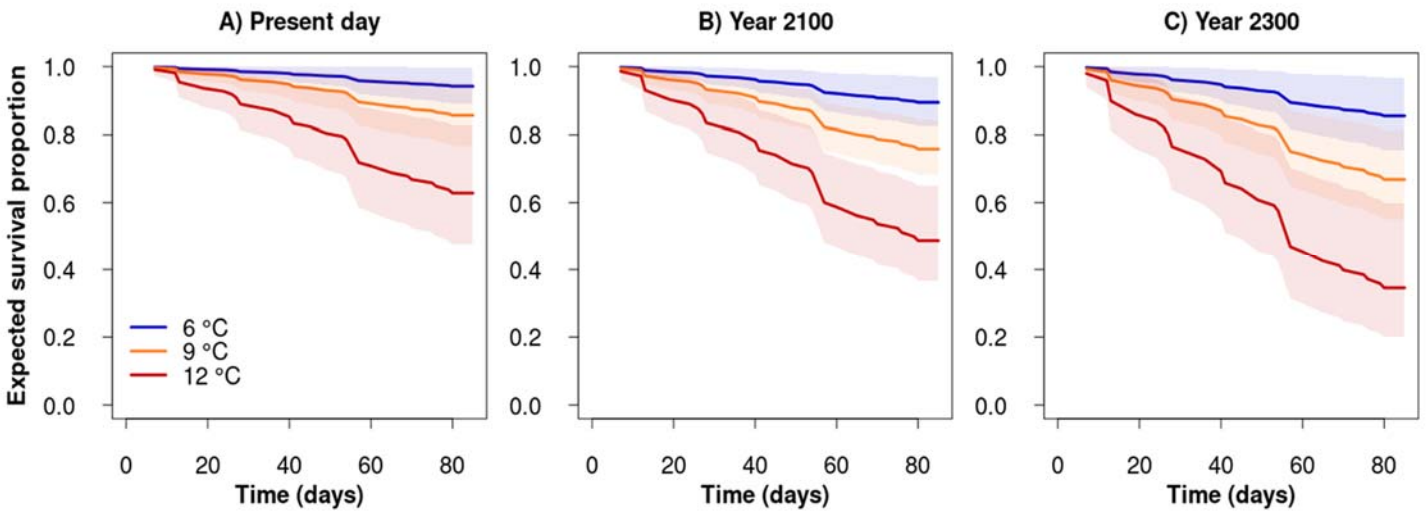

Figure. 6 Thresholds for Atlantic sea scallop growth, persistence, and mortality according to predictive models of seawater temperature and $\Omega_{calcite}$. Thresholds were generated from linear mixed effects models that found significant effects of temperature and $\Omega_{calcite}$ on calcification rate and survival probability. 'Mortality' was assigned when temperature and $\Omega_{calcite}$ had a lethal dosing effect on 50% of the population or greater (LD_{50}). 'Persistence (survival without growth)' was assigned when predicted mortality was <50%, but calcification was not predicted to occur. 'Growth' was assigned when mortality was <50% and calcification was predicted to occur.

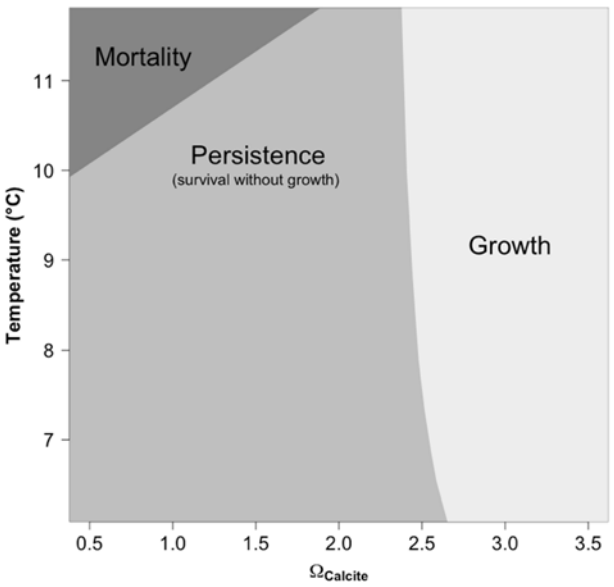

364

Discussion

Respiration rate declined significantly in response to OA, which is consistent with previous observations of negative effects of OA on respiration rates (Pörtner et al. 1998; Melatunan et al. 2011; Liu and He 2012; Zhao et al. 2017). In contrast, four bivalve species (*Argopecten irradians, Crassostrea virginica, Mytilus edulis,* and *Mercenaria mercenaria*) exhibited either no response, or enhanced respiration, under lower pH conditions (Stevens and Gobler 2018). However, these species are adapted to a wider thermal range than Atlantic sea scallops (Shumway and Parsons 2006) and inhabit more variable pH environments (Cyronak et al. 2018), so their metabolic pathways may be better suited to higher temperatures and lower pH. The observed reduction in sea scallop respiration rate under OA may be due to either hypercapnic suppression of metabolism, or reduced activity levels. Hypercapnia occurs when excessive CO_2 builds up in the bloodstream or hemolymph of animals, and can occur when bivalves are exposed to high environmental pCO_2 (Michaelidis et al. 2005). The glycolytic enzymes that assist with oxygen uptake may show reduced function when haemolymph pH is low (Pörtner et al. 1998; Michaelidis et al. 2005). The observed decline in respiration rate in response to OA may therefore arise from a reduction in oxygen affinity. Alternatively, reduced respiration rate may be caused by a change in oxygen demand due to decreased activity (Lefevre 2016). Protein synthesis and ion transport processes can be reduced under OA (Pan et al. 2015; Frieder et al. 2017). Additional research is necessary to ascertain whether reductions in metabolic rate are due to reduced oxygen demand or uptake in this species.

Warming did not affect respiration rate (Fig. 1a). Ectothermic organisms exist within a window of temperatures called a thermal tolerance zone. As temperature did not elicit a response, the temperatures encompassed by the experimental treatments span the thermal

388 tolerance of the scallops, although the negative survivorship trends suggest that these
389 temperatures were not necessarily optimal. Respiration rates were measured close to the end of
390 the experiment, so respiration rate was only measured on survivors. Therefore, a metabolic
391 response to temperature may have been masked due to the mortality of individuals that exhibited
392 this response. The Georges Bank Atlantic sea scallop population experiences a temperature range
393 of 5 to 14 °C, but rarely experiences temperatures exceeding 12 °C for extended periods
394 (Butman and Beardsley 1987). Future warming may increase the duration that scallops are
395 exposed to temperatures at the upper end of this range.

396 All aspects of the EPF carbonate system were affected by seawater acidification, but none
397 were affected by temperature. Extrapallial fluid pH declined linearly to OA, but with a shallower
398 slope than the declining seawater pH (Fig. 2a), which caused EPF pH to approach seawater pH in
399 the year 2300 pCO_2 treatment. The EPF pH of three bivalve species (*Mercenaria mercenaria,*
400 *Crassostrea virginica*, *Mytilus edulis*) ranged from 7.33 ± 0.15 s.d. to 7.41 ± 0.17 under ambient
401 seawater pH (pH 7.91 ± 0.11 s.d.) (Crenshaw 1972). This range is similar to the EPF pH of
402 Atlantic sea scallops measured under the present-day pCO_2 treatment (7.30 ± 0.39 s.d.). The EPF
403 pH of the tropical clam *Tridacna squamosa* is much higher (range = 7.70 – 7.80) than the EPF
404 pH measured here or previously. *Tridacna squamosa* harbors photosynthetic symbionts within its
405 mantle that likely elevate EPF pH via photosynthetic drawdown of aqueous CO_2 (Ip et al. 2005).
406 Two prior studies have investigated the response of EPF pH to OA. The king scallop *Pecten*
407 *maximus* maintained a constant offset between seawater and EPF pH across all pCO_2 treatments
408 under control temperatures (Cameron et al. 2019). This contrasts the observation in the present
409 study that Atlantic sea scallop EPF pH decreases at a gentler slope than seawater pH under OA,
410 suggesting that sea scallops invest greater effort in removing protons from their EPF than king

411 scallops when exposed to OA. Larval mussels (*Mytilus edulis*) elevated EPF pH above seawater
412 pH when exposed to OA (Ramesh et al. 2017). The highest degree of pH regulation is shown in
413 the larval *M. edulis.* Larval bivalves generally build their shells entirely from the aragonite
414 polymorph of $CaCO_3$ (Waldbusser et al. 2015), whereas adult bivalves typically construct their
415 shells from the less soluble calcite polymorph or a combination of the calcite and aragonite
416 polymorphs (Lowenstam and Weiner 1989). Larvae may invest a greater proportion of
417 organismal energy into elevation of EPF pH to aid the formation and preservation of aragonite
418 shell, due to its higher solubility than the calcite that is produced by most adult bivalves and the
419 importance of rapid shell production at the larval stage.
420 Extrapallial fluid DIC and TA both increased dramatically in response to OA (Fig. 2b &
421 c). The EPF DIC of three bivalve species (*Mercenaria mercenaria, Crassostrea virginica*,
422 *Mytilus edulis*) was nearly double that of ambient seawater (Crenshaw 1972). Although this was
423 observed for most scallops exposed to present-day pCO_2, there was a high degree of inter-
424 specimen variability. Extrapallial fluid DIC fluctuates over time within individuals (Crenshaw et
425 al. 1972; Stemmer et al. 2019), possibly due to cyclic transport of DIC towards the site of
426 calcification (Stemmer et al. 2019). The high variation in extrapallial fluid DIC observed here
427 could therefore be due to variability in calcification cycles amongst individuals. DIC
428 concentration may occur through several pathways. Ion channels concentrate carbonate and
429 bicarbonate derived from seawater (Sillanpää et al. 2018) or through metabolic pathways (Zhao
430 et al. 2018) in calcifying compartments. Decreased flushing rates during closed-shell respiration
431 can also cause a build-up of metabolic CO_2 in tissues and extracellular fluids (Michaelidis et al.
432 2005), which may result in a build-up of CO_2 in the EPF. Shell dissolution is a mechanism by
433 which bivalves may buffer extracellular pH changes (Crenshaw and Neff 1969), and this may

increase EPF DIC. Future research should be directed towards establishing the source of EPF DIC to ascertain whether the elevated DIC observed under OA arises from active carbon concentration in support of calcification, increased respiration of CO_2 into the EPF, or shell dissolution in support of regulating pH within extracellular fluids.

Total alkalinity (TA) is a measure of the proton-neutralizing capacity of a fluid and increases when protons are removed from that fluid (Dickson 1981). Modifying calcification site pH via proton removal has been identified as a mechanism to facilitate calcification in a range of calcifying taxa (de Beer and Larkum 2002; Cohen and Holcomb 2009; Toyofuku et al. 2017; Sutton et al. 2018; Liu et al. 2020). Although scallop EPF pH was typically lower than seawater pH, that does not discount the potential role of proton removal from the EPF in creating an environment that aids calcification. This is supported by the decline in ΔpH observed in response to acidification, and by the observation of rapid pH fluctuation within the extrapallial fluid of other bivalve species (Stemmer et al. 2019), which is consistent with proton pumping activity. Assuming that EPF chemistry is influenced by the bivalve's surrounding seawater–as supported by the influence of seawater chemistry on the elemental composition of bivalve biominerals (Lorens and Bender 1980; Checa et al. 2007)–the difference between EPF TA and seawater TA (ΔTA) should approximate the net number of protons removed from the EPF. The ΔTA increased under OA (Fig. 2c; Fig. S5b), suggesting that proton removal increases with increasing OA which may be energetically expensive.

Extrapallial fluid [CO_3^{2-}] increased significantly under OA stress, and was higher on average than seawater [CO_3^{2-}] in the year 2300 pCO_2 treatment (Fig. 2D). This illustrates that Atlantic sea scallops, and potentially bivalves in general, increase [CO_3^{2-}] of their EPF to mitigate the effects of CO_2-induced OA. It should be noted that the benefit of EPF [CO_3^{2-}] relies

on the scallops' ability to incorporate that CO_3^{2-} into $CaCO_3$ shell, and any resilience conferred by this control over EPF [CO_3^{2-}] may be offset by dissolution of the scallop's external shell (Ries et al. 2016) under low seawater pH.

Calcification rate was affected by the interactive effects of OA and warming. Under present-day pCO_2, calcification was fastest in the highest temperature treatment, but the calcification rates of scallops at this temperature were the most negatively affected by OA (Fig. 3). Furthermore, the effects of temperature completely inverted under the highest pCO_2 treatment, with sea scallops calcifying fastest in the lowest temperature treatment.This highlights the importance of investigating the combined effects of multiple global change stressors. Atlantic sea scallops began exhibiting net shell dissolution at $\Omega_{calcite}$ well above 1 (Fig. 3)—the chemical divide between the dissolution ($\Omega_{calcite} < 1$) and precipitation ($\Omega_{calcite} > 1$) of inorganic calcite—suggesting that predicted decline in $\Omega_{calcite}$ coupled with increased seawater temperature over the 21st century will be highly detrimental to this species. Other bivalve species (*Mercenaria spp.*, *Crassostrea gigas*) also exhibit shell dissolution above their calcium carbonate saturation threshold (Waldbusser et al. 2010; Barton et al. 2012), indicating that high seawater Ω is particularly important for this group.

There was a positive correlation between rates of respiration and calcification under the present-day pCO_2 treatment, but not under OA conditions (Fig. 1B). Bivalve shell formation is under strong biological control (Marie et al. 2008). Progressive impairment of metabolic function with increasing OA may be partly responsible for the decline in calcification rate under these conditions. Although a correlation was not found between calcification and respiration rates under OA treatments, a trend may be masked by the observed dissolution of external shell. OA negatively affects calcification rate and metabolic rate in other bivalve species (Zhao et al. 2017),

480 but this is the first study to show a direct link between oxygen consumption and calcification
481 rate. The energetic cost of calcification has not been well constrained in bivalves. Observed
482 relationships between rates of calcification and food consumption indicate that calcification can
483 be energetically expensive (Palmer 1992). Additionally, a shift in the dominant mineralogy of
484 *Mytilus californianus* from aragonite to calcite in response to acidification over decadal
485 timescales suggests that switching to a less soluble calcium carbonate polymorph may conserve
486 energy by decreasing shell maintenance costs (Bullard et al. 2021). The direct link between rates
487 of calcification and respiration observed here provides further evidence that calcification is
488 energetically costly. A positive correlation was also observed between calcification rate and EPF
489 pH (Fig. 4). This reveals the importance of maintaining optimal pH conditions within sea scallop
490 EPF. The activity of carbonic anhydrase, one of the enzymes involved in calcification, is
491 inhibited under low pH (Kernohan 1965). The ability of scallops to maintain a sufficiently high
492 pH in their EPF to support enzyme function may therefore play a role in their response to OA.
493 OA and warming (Fig. 5) had additive negative effects on survivorship. This is consistent
494 with previous observations of additive effects of these stressors (Talmage and Gobler 2011;
495 Stevens and Gobler 2018) and decreased survivorship in bivalves exposed to warming (Beukema
496 et al. 2009) and acidification (Green et al. 2009). This observation suggests that OA lowers the
497 upper thermal tolerance of Atlantic sea scallops, as shown previously in the Sydney rock oyster
498 *Saccostrea glomerata* (Parker et al. 2017). Across their range Atlantic sea scallops can tolerate
499 temperatures of 1.2 – 18 °C (Hart and Chute 2004). Although scallops on Georges Bank can
500 experience temperatures of up to 15 °C, they typically do not experience temperatures higher
501 than 12 °C for more than 30 days (Butman and Beardsley 1987). The observed negative effect of
502 thermal stress on survivorship suggests that sea scallops may experience increased mortality

503 under future warming scenarios, especially as waters become increasingly acidified. The
504 Atlantic sea scallop fishery is currently valued at over $500 million USD (NMFS 2017) and
505 modeling outputs suggest that OA will cause declines in scallop biomass, yield and associated
506 profits (Cooley et al. 2015). Our results suggest that warming may cause more losses than
507 previously predicted owing to the interactive negative effects of OA and warming on sea scallop
508 growth and mortality. This highlights the importance of investigating the effects of multiple
509 global change stressors on commercially valuable marine species.
510 This study provides insights into the mechanisms by which global change affects Atlantic sea
511 scallops. Scallops used a combination of proton removal and DIC elevation to increase the
512 concentration EPF [CO_3^{2-}] —a process that was enhanced under OA. However, calcification
513 rates declined under OA conditions (Fig. 3), despite increasing EPF [CO_3^{2-}]. The inverse
514 relationship between EPF [CO_3^{2-}] and calcification rate may exist because (1) metabolic activity
515 was greatest in the present-day pCO_2 treatment, (2) high rates of calcification at the site of
516 calcification were offset by equally high rates of shell dissolution in OA treatments, and/or (3)
517 the high rates of calcification in the present-day pCO_2 treatment reduced EPF [CO_3^{2-}] via
518 drawdown of DIC. The bivalve EPF contains a sophisticated toolkit for producing
519 mineralized structures (Addadi et al. 2006; Feng et al. 2017; Jaramillo-Martínez et al. 2019; Jin
520 et al. 2019; Song et al. 2019). Activating and maintaining this requires energy (Frieder et al.
521 2017) and an environment that supports protein function (Kanmani and Thiyagarajan 2020),
522 which may be inhibited under low pH (Kernohan 1965). Although EPF TA elevation suggests
523 that there is sufficient energy available for proton removal under OA, low calcification rates
524 suggest that scallops cannot convert excess [CO_3^{2-}] into shell and/or are unable to maintain this
525 shell due to dissolution. This implies that any beneficial effects of proton removal are

526 insufficient to offset the negative effects of OA on calcification. Further, our results suggest that
527 reduced metabolic function under OA prevents Atlantic sea scallops from keeping pace with the
528 increased energetic cost of maintaining an environment in the EPF that aids calcification. The
529 high mortality rate observed under OA further supports the assertion that CO_2-induced inhibition
530 of metabolic function compounds the challenge of forming shell in acidified conditions.
531

532 **References**

533 Addadi, L., D. Joester, F. Nudelman, and S. Weiner. 2006. Mollusk Shell Formation: A Source
534 of New Concepts for Understanding Biomineralization Processes. Chemistry. **12(4):** 980 – 987.
535 doi: 10.1002/chem.200500980
536
537 Al-Horani, F. A., S. M. Al-Moghrabi, and D. de Beer. 2003. The mechanism of calcification and
538 its relation to photosynthesis and respiration in the scleractinian coral Galaxea fascicularis.
539 Marine Biology. **14:** 419 – 426. doi:
540
541 Barton, A., B. Hales, G. G. Waldbusser, C. Langdon, and R. A. Feely. 2012. The Pacific oyster,
542 *Crassostrea gigas,* shows negative correlation to naturally elevated carbon dioxide levels:
543 Implications for near-term ocean acidification effects. Limnology and Oceanography. **57(3):** 698
544 – 710. doi: 10.4319/lo.2012.57.3.0698
545
546 Bates, N. R., M. H. P. Best, K. Neely, R. Garley, A. G. Dickson, and R. J. Johnson. 2012.
547 Detecting anthropogenic carbon dioxide uptake and ocean acidification in the North Atlantic
548 Ocean. Biogeosciences Discussions. **9:** 989 – 1019. doi: 10.5194/bg-9-2509-2012

549

550 Beukema, J. J., R. Dekker, and J. M. Jansen. 2009. Some like it cold: populations of the tellinid

551

552

553

554

555 Brennand, H. S., N. Soars, S. A. Dworjanyn, A. R. Davis, and M. Byrne. 2010. Impact of Ocean

556 Warming and Ocean Acidification on Larval Development and Calcification in the Sea Urchin

557 Tripneustes gratilla. PloS One. **5(6):** e11372. doi: 10.1371/journal.pone.0011372

558

559 Brooks, S. P. J. and K. B. Storey, 1997. Glycolytic controls in estivation and anoxia: A

560 comparison of metabolic arrest in land and marine molluscs. Comparative Biochemistry and

561 Physiology Part A: Physiology. **118(4):** 1103 – 1114. doi: 10.1016/S0300-9629(97)00237-5

562

563 Bullard, E. M., I. Torres, T. Ren, O. A. Graeve, and K. Roy. 2021. Shell mineralogy of a

564 foundational marine species *Mytilus californianus,* over half a century in a changing ocean.

565 PNAS. **118(3):** e2004769118. doi: 10.1073/pnas.2004769118

566 Butman, B., and R. C. Beardsley. 1987. Long-Term Observations on the Southern Flank of

567 Georges Bank. Part I: A Description of the Seasonal Cycle of Currents, Temperature,

568 Stratification, and Wind Stress. Journal of Physical Oceanography. **17(3):** 367 – 384. doi:

569 10.1175/1520-0485(1987)017<0367:LTOOTS>2.0.CO;2

570

571 Cameron, L. P., C. E. Reymond, F. Müller-Lundin, I. Westfield, J. H. Grabowski, H.
572 Westphal, and J. B. Ries. 2019. Effects of temperature and ocean acidification on the
573 extrapallial fluid pH, calcification rate, and condition factor of the king scallop *Pecten*
574 *maximus*. Journal of Shellfish Research. **38(3):** 763 – 777. doi: 10.2983/035.038.0300
575
576 Checa, A. G., C. Jiménez-Lópe, A. Rodríguez-Navarro, and J. P. Machado. 2007. Precipitation
577 of aragonite by calcitic bivalves in Mg-enriched marine waters. Marine Biology. **150:** 819 – 827.
578 doi: 10.1007/s00227-006-0411-4
579
580 Cohen, A. L., and M. Holcomb. 2009. Why Corals Care About Ocean Acidification: Uncovering
581 the Mechanism. Oceanography. **22(4).** doi: 10.5670/oceanog.2009.102
582
583 Crain, C. M., K. Kroeker, and B. S. Halpern. 2008. Interactive and cumulative effects of multiple
584 human stressors in marine systems. Ecology Letters. **11(12):** 1304 – 1315. doi: 10.1111/j.1461-
585 0248.2008.01253.x
586
587 Crenshaw, M. A. 1972. The inorganic composition of molluscan extrapallial fluid. Biological
588 Bulletin. **143(3):** 506 – 512. doi:
589
590 Crenshaw, M. A., and J. M. Neff. 1969. Decalcification at the Mantle-Shell Interface in
591 Molluscs. Integrative and Comparative Biology. **9(3):** 881 – 885. doi: 10.1093/icb/9.3.881
592

593 Cyronak, T., A. J. Andersson, S. D'Angelo, P. Bresnahan, C. Davidson, C. Griffin, T.
594 Kindeberg, J. Pennise, Y. Takeshita, and M. White. 2018. Short-Term Spatial and Temporal
595 Carbonate Chemistry Variability in Two Contrasting Seagrass Meadows: Implications for pH
596 Buffering Capacities. Estuaries and Coasts. **41:** 1282 – 1296. doi: 10.1007/s12237-017-0356-5
597
598 De Beer, D., and A. W. D. Larkum. 2002. Photosynthesis and calcification in the calcifying
599 algae *Halimeda discoidea* studied with microsensors. Plant, Cell & Environment. **24(11):** 1209 –
600 1217. doi: 10.1046/j.1365-3040.2001.00772.x
601
602 De Wit, P., E. Durland, A. Ventura, and C. J. Langdon. 2018. Gene expression correlated with
603 delay in shell formation in larval Pacific oyster (*Crassostrea gigas*) exposed to experimental
604 ocean acidification provides insights into shell formation mechanisms. BMC Genomics. **19:**160.
605 doi: 10.1186/s12864-018-4519-y
606
607 Dickson, A. G. 1981. An exact definition of total alkalinity and a procedure for the estimation of
608 alkalinity and total inorganic carbon from titration data. Deep Sea Research Part A.
609 Oceanographic Research Papers. **28(6):** 609 – 623. doi: 10.1016/0198-0149(81)90121-7.
610
611 Dickson, A. G. 1990. Standard potential of the reaction: $AgCl(s) + 12H_2(g) = Ag(s) + HCl(aq)$,
612 and the standard acidity constant of the ion HSO_4^- in synthetic sea water from 273.15 to 318.15
613 K. The Journal of Chemical Thermodynamics. **22(2):** 113 – 127. doi: 10.1016/0021-
614 9614(90)90074-Z
615

Doney, S. C., V. J. Fabry, R. A. Feely, and J. A. Kleypas2009. Ocean Acidification: The Other CO_2 Problem. Annual Review of Marine Science. **1:** 169 – 192. doi: 10.1146/annurev.marine.010908.163834

Dow, K. and Downing, T. E. 2016. The atlas of climate change: mapping the world's greatest challenge. USA: University of California Press.

Feng, D., Q. Li, H. Yu, L. Kong, and S. Du. 2017. Identification of conserved proteins from diverse shell matrix proteome in Crassostrea gigas: characterization of genetic bases regulating shell formation. Scientific Reports. Doi: 10.1038/srep45754

Frieder, C. A., S. L. Applebaum, T.-C. F. Pan, D. Hedgecock, and D. T. Manahan. 2017. Metabolic cost of calcification I bivalve larvae under experimental ocean acidification. ICES Journal of Marine Science. **74(4):** 941 – 954. doi: 10.1093/icesjms/fsw213

Frossard, J. and O. Renaud. 2019. permuco: Permutation tests for regression, (repeated measures) ANOVA/ANCOVA and comparison of signals. R package version 1.10. https://www.rdocumentation.org/packages/permuco/versions/1.1.0

Gazeau, F., C. Quiblier, J. M. Jansen, J.-P. Gattuso, J. J. Middelburg, and C. H. R. Heip. 2007. Impact of elevated CO_2 on shellfish calcification. Geophysical Research Letters. **34(7):** L07603. doi: 10.1029/2006GL028554

639 Gazeau, F., L. Parker, S. Comeau, J.-P. Gattuso, W. A. O'Connor, S. Martin, H.-O. Pörtner, and
640 P. M. Ross. 2013. Impacts of ocean acidification on marine shelled molluscs. Marine Biology.
641 **160:** 2207 – 2245. doi: 10.1007/s00227-013-2219-3
642
643 Gillooly, J. F., J. H. Brown, G. B. West, V. M. Savage, E. L. and Charnov. 2001. Effects of Size
644 and Temperature on Metabolic Rate. Science. **293(5538):** 2248 – 2251. doi:
645
646
647 Green, M. A., G. G. Waldbusser, S. L. Reilly, K. Emerson, and S. O'Donnell. 2009. Death by
648 dissolution: Sediment saturation state as a mortality factor for juvenile bivalves. Limnology and
649 Oceanography. **54(4):** 1037 – 1047. doi: 10.4319/lo.2009.54.4.1037
650
651 Gunderson, A. R., E. J. Armstrong, and J. H. Stillman. 2016. Multiple Stressors in a Changing
652 World: The Need for an Improved Perspective on Physiological Responses to the Dynamic
653 Marine Environment. Annual Review of Marine Science. **8:** 357 – 378. doi: 10.1146/annurev-
654 marine-122414-033953
655
656 Harney, E., S. Artigaud, P. Le Souchu, P. Miner, C. Corporeau, H. Essid, V. Pichereau, and F. L.
657 D. Nunes. 2016. Non-additive effects of ocean acidification in combination with warming on the
658 larval proteome of the Pacific oyster, *Crassostrea gigas.* Journal of Proteomics. **1(135):** 151 –
659 161. doi: 10.1016/j.prot.2015.12.001
660

Hart, D. R., and A. S. Chute. 2004. Essential Fish Habitat Source Document: Sea Scallop, *Placopecten magellanicus,* Life History and Habitat Characteristics. NOAA Technical Memorandum NMFS-NE-189.

Hart, D. R., and P. J. Rago. 2011. Long-Term Dynamics of U.S. Atlantic Sea Scallop Placopecten magellanicus Populations. Orth American Journal of Fisheries Management. **26(2):** 490 – 501. doi: 10.1577/M04-116.1

Hattan, S. J., T. M. Laue, and N. D. Chasteen. 2000. Purification and Characterization of a Novel Calcium-binding Protein from the Extrapallial Fluid of the Mollusc, Mytilus edulis. Journal of Biological Chemistry. **276:** 4461 – 4468. doi: 10.1074/jbc.M006803200

Helm, M. M., and N. Bourne. 2004. Hatchery culture of bivalves: a practical manual. FAO Fisheries Aquaculture Tech Papers Issue 471 of FAO fisheries technical paper, Food and Agriculture Organization. California, USA.

Ip, Y. K., A. M. Loong, K. C. Hiong, W. P. Wong, S. F. Chew, K. Reddy, B. Sivaloganathan, and J. S. Ballantyne. 2005. Light Induces an Increase in the pH of and a Decrease in the Ammonia Concentration in the Extrapallial Fluid of the Giant Clam Tridacna squamosa. Physiological and Biochemical Zoology. **79(3):** 656 – 664. doi: 10.1086/501061

IPCC, 2019: IPCC Special Report on the Ocean and Cryosphere in a Changing Climate [H.-O. Pörtner, D. C. Roberts, V. Masson-Delmotte, P. Zhai, M. Tignor, E. Poloczanska, K.

684 Mintenbeck, A. Alegría, M. Nicolai, A. Okem, J. Petzold, B. Rama, N. M. Weyer (eds.)]. In
685 press.
686
687 Jaramillo-Martínez, S., C. Vargas-Requena, C. Rodríguez-Gónzalez, A. Hernández-Santoyo, and
688 I. Olivas-Armendáriz. 2019. Effect of extrapallial protein of Mytilus californianus on the process
689 of in vitro biomineralization of chitosan scaffolds. Heliyon. **5(8):** e02252. doi:
690 10.1016/j.heliyon.2019.e02252
691
692 Jin, C., J. Zhao, J. Pu, X. Liu, and J. Li. 2019. Hichin, a chitin binding protein is essential for the
693 self-assembly of organic frameworks and calcium carbonate during shell formation. International
694 Journal of Biological Macromolecules. **15(135):** 745 – 751. doi: 10.1016/j.ijbiomac.2019.05.205
695
696 Kanmani, C. R., and V. Thiyagarajan. 2020. Molecular adaptation of molluscan
697 biomineralization to high-CO_2 oceans – The known and the unknown. Marine Environmental
698 Research. **155:** 104883. doi: 10.1016/j.marenvres.2020.104883
699
700 Kernohan, J. C. 1965. The pH-activity curve of bovine carbonic anhydrase and its relationship to
701 the inhibition of the enzyme by anions. Biochimica et Biophysica Acta (BBA) – Enzymology
702 and Biological Oxidation. **96(2):** 304 – 317. doi: 10.1016/0926-6593(65)90014-7
703
704 Kherad-Pajouh, S. 2010. An exact permutation method for testing any effect in balanced and
705 unbalanced fixed effect ANOVA. Computational Statistics & Data Analysis. Doi:
706 10.1016/j.csda.2010.02.015

Ko, G. W. K., R. Dineshram, C. Campanati, V. B. S. Chan, J. Havenhand, and V. Thiyagarajan. 2014. Interactive Effects of Ocean Acidification, Elevated Temperature, and Reduced Salinity on Early-Life Stages of the Pacific Oyster. Environmental Science & Technoloy. **48(17):** 10079 – 10088. doi: 10.1021/es501611u

Kroeker, K. J., B. Gaylord, T. M. Hill, J. D. Hosfelt, S. H. Miller, and E. Sanford. 2014. The Role of Temperature in Determining Species' Vulnerability to Ocean Acidification: A Case Study Using *Mytilus galloprovincialis*. PloS One. **9(7):** e100353. doi: 10.1371/journal.pone.0100353

Lannig, G., S. Eilers, H. O. Pörtner, I. M. Sokolova, and C. Bock. 2010. Impact of Ocean Acidification on Energy Metabolism of Oyster, Crassostrea gigas – Changes in Metabolic Pathways and Thermal Response. Marine Drugs. **8(8):** 2318 – 2339. doi: 10.3390/md8082318

Lee, K., T.-W. Kim, R. H. Byrne, F. J. Millero, R. A. Feely, and L. Yong-Ming. 2010. The universal ratio of boron to chlorinity for the North Pacific and North Atlantic oceans. Geochimica et Cosmochimica Acta. **74(6):** 1801 – 1811. doi: 10.1016/j.gca.2009.12.027

Lefevre, S. 2016. Are global warming and ocean acidification conspiring against marine ectotherms? A meta-analysis of the respiratory effects of elevated temperature, high CO_2 and their interaction. Conservation Physiology. **4(1):** cow009. doi: 10.1093/conphys/cow009

Liu, W. and M. He. 2012. Effects of ocean acidification on the metabolic rates of three species of bivalve from southern coast of China. Chinese Journal of Oceanology and Limnology. **30:** 206. doi:

Liu, Y.-W., J. N. Sutton, J. B. Ries, and R. A. Eagle. 2020. Regulation of calcification site pH is a polyphyletic but not always governing response to ocean acidification, Science Advances, **6(5):** eaax1314. doi: 10.1126/sciadv.aax1314

Lorens, R. B. and M. L. Bender. 1980. The impact of solution chemistry on *Mytilus edulis* calcite and aragonite. Geochimica et Cosmochimica Acta. **44(9):** 1265 – 1278. doi: 10.1016/0016-7037(80)90087-3

Lowenstam, H. A. and S. Weiner. 1989. On Biomineralization. UK: Oxford University Press

753 Ma, Z., J. Huang, J. Sun, G. Wang, C. Li, L. Xie, and R. Zhang. 2007. A Novel Extrapallial
754 Fluid Protein Controls the Morphology of Nacre Lamellae in the Pearl Oyster, *Pinctada fucata*.
755 Journal of Biological Chemistry. **282(32):** 23253 – 23263. doi: 10.1074/jbc.M700001200
756
757 Marie, B., G. Luquet, L. Bédouet, C. Milet, N. Guichard, D. Medakovic, and Marin, F. 2008.
758 Nacre Calcification in the Freshwater Mussel *Unio pictorum:* Carbonic Anhydrase Activity and
759 Purification of a 95 kDa Calcium-Binding Glycoprotein. ChemBioChem. **9(15):** 1515 – 1523.
760 doi: 10.1002/cbic.200800159.
761
762 McCulloch, M., J. Falter, J. Trotter, J. and P. Montagna. 2012. Coral resilience to ocean
763 acidification and global warming through pH up-regulation. Nature Climate Change. **2:** 623 –
764 627, doi:
765
766 Melatunan, S., P. Calosi, S. D. Rundle, A. J. Moody, and S. Widdicombe. 2011. Exposure to
767 Elevated Temperature and pCO_2 Reduces Respiration Rate and Energy Status in the Periwinkle
768 *Littorina littorea*. Physiological and Biochemical Zoology. **84(6):** 583 – 594. doi:
769 10.1086/662680
770
771
772
773
774

775 Millero, F. J. 2007. The Marine Inorganic Carbon Cycle. Chemical Reviews. **107(2):** 308 – 341.
776 doi: 10.1021/cr0503557
777
778 Misogianes, M. J. and N. D. Chasteen. 1979. A chemical and spectral characterization of the
779 extrapallial fluid of *Mytilus edulis*. Analytical Biochemistry. **100(2):** 324 – 334. doi:
780 10.1016/0003-2697(79)90236-7
781
782 Morita, M., R. Suwa, A. Iguchi, and M. Nakamura. 2010. Ocean acidification reduces sperm
783 flagellar motility in broadcast spawning reef invertebrates. Zygote. **18(2):** 103 – 107.
784 doi: 10.1017/S0967199409990177
785
786 de Nooijer, L. J., T. Toyofuku, and H. Kitazato. 2009. Foraminifera promote calcification by
787 elevating their intracellular pH. Proceedings of the National Academy of Sciences of the United
788 States of America. **106(36):** 15374 – 15378, doi: 10.1073/pnas.0904306106
789
790 Palmer, A. R. 1992. Calcification in marine molluscs: how costly is it? Proceedings of the
791 National Academy of Sciences of the United States of America. **89(4):** 1379 – 1382. doi:
792 10.1073/pnas.89.4.1379
793
794 Pan, T.-C. F., S. C. Applebaum, and D. T. Manahan. 2015. Experimental ocean acidification
795 alters the allocation of metabolic energy. Proceedings of the National Academy of Sciences of
796 the United States of America. **112(15):** 4696 – 4701. doi: 10.1073/pnas.141697112

Parker, L. M., P. M. Ross, and W. A. O'Connor. 2010. Comparing the effect of elevated pCO_2 and temperature on the fertilization and early development of two species of oysters. Marine Biology. **157:** 2435 – 2452. doi: 10.1007/s00227-010-1508-3

Parker, L. M., E. Scanes, W. O'Connor, R. A. Coleman, M. Byrne, H. O. Pörtner, and P. M. Ross. 2017. Ocean acidification narrows the acute thermal and salinity tolerance of the Sydney rock oyster *Saccostrea glomerata.* Marine Pollution Bulletin. **112(1-2):** 263 – 271. doi: 10.1016/j.marpolbul.2017.06.052

Pershing, A. J., M. A. Alexander, C. M. Hernandez, L. A. Kerr, A. Le Bris, K. E. Mills, J. A. Nye, N. R. Record, H. A. Scannell, J. D. Scott, G. D. Sherwood, and A. C. Thomas. 2015. Slow adaptation in the face of rapid warming leads to collapse of the Gulf of Maine cod fishery. Science. **350(6262):** 809 – 812. doi: 10.1126/science.aac9819

Pörtner, H. O., A. Reipschläger, and N. Heisler. 1998. Acid-base regulation, metabolism and energetics in *Sipunculus nudus* as a function of ambient carbon dioxide level. Journal of Experimental Biology. **201:** 43-55.

Pörtner, H. O. 2008. Ecosystem effects of ocean acidification in times of ocean warming: a physiologist's view. Marine Ecology Progress Series. **373:** 203 – 217. doi: 10.3354/meps07768

819 Pörtner, H. O. and A. P. Farrell. 2008. Physiology and Climate Change. Science. **322(5902):** 690
820 – 692. doi: 10.1126/science.1163156
821
822 Ramesh, K., M. Y. Hu, J. Thomsen, M. Bleich, and F. Melzner. 2017. Mussel larvae modify
823 calcifying fluid carbonate chemistry to promote calcification. Nature Communications. **8:** 1709.
824 doi:
825
826 Reymond, C. E., A. Lloyd, D. I. Kline, S. G. Dove, and J. M. Pandolfi. 2012. Decline in growth
827 of foraminifer *Marginopora rossi* under eutrophication and ocean acidification scenarios. **19(1):**
828 291 – 302. doi: 10.1111/gcb.12035
829
830 Ries, J. B., A. L. Cohen, and D. C. McCorkle. 2009. Marine calcifiers exhibit mixed responses to
831 CO_2-induced ocean acidification. Geology. **37(12):** 1131 – 1134. doi: 10.1130/G30210A.1
832
833 Ries, J. B. 2011. A physicochemical framework for interpreting the biological calcification
834 response to CO_2-induced ocean acidification. Geochimica et Cosmochimica Acta. **75(14):** 4053
835 – 4064. doi: 10.1016/j.gca.2011.04.025
836
837 Ries, J. B., M. N. Ghazaleh, B. Connolly, I. Westfield, and K. D. Castillo. 2016. Impacts of
838 seawater saturation state (Ω_A = 0.4 – 4.6) and temperature (10, 25 °C) on the dissolution kinetics
839 of whole-shell biogenic carbonates. Geochimica et Cosmochimica Acta. **192:** 318 – 337. doi:
840 10.1016/j.gca.2016.07.001
841

842 Rodolfo-Metalpa, R., F. Houlbrèque, È. Tabmuttè, F. Boisson, C. Baggini, F. P. Patti, R. Jeffree,
843 M. Fine, A. Foggo, J.-P. Gattuso, and J. M. Hall-Spencer. 2011. Coral and mollusk resistance to
844 ocean acidification adversely affected by warming. Nature Climate Change. **1:** 308 – 312. doi:
845
846
847 Roy, R. N., L. N. Roy, K. M. Vogel, C. Porter-Moore, T. Pearson, C. E. Good, F. J. Millero, and
848 D. M. Campbell. 1993. The dissociation constants of carbonic acid in seawater at salinities 5 to
849 45 and temperatures 0 to 45°C. Marine Chemistry. **44(2-4):** 249 – 267. doi: 10.1016/0304-
850 4203(93)90207-5
851
852 Sanders, M. B., T. P. Bean, T. H. Hutchinson, and W. J. F. Le Quesne. 2013. Juvenile King
853 Scallop, *Pecten maximus*, Is Potentially Tolerant to Low Levels of Ocean Acidification When
854 Food Is Unrestricted. PloS One. **8(9):** e74118. doi: 10.1371/journal.pone.0074118
855
856 Shumway, S. E. and G. J. Parsons. 2006. Scallops: biology, ecology, and aquaculture. Elsevier.
857
858 Sillanpää, J. K., H. Sundh, and K. Sundell. 2018. Calcium transfer across the outer mantle
859 epithelium in the Pacific oyster, *Crassostrea gigas.* Proceedings of the Royal Society B.
860 **285(1891):** 20181676. doi: 10.1098/rspb.2018.1676
861
862 Song, X., Z. Liu, L. Wang, and L. Song. 2019. Recent Advances of Shell Matrix Proteins and
863 Cellular Orchestration in Marine Molluscan Shell Biomineralization. Frontiers in Marine
864 Science. **6:** 41. doi: 10.3389/fmars.2019.00041

Stemmer, K., T. Brey, M. S. Gutbrod, M. Beutler, B. Schalkhausser, and D. de Beer. 2019. *In Situ* measurements of pH, Ca^{2+}, and DIC dynamics within the extrapallial fluid of the ocean quahog *Arctica islandica*. Journal of Shellfish Research. **38(1):** 71 – 78, doi: 10.2983/035.038.0107

Stevens, A. M. and C. J. Gobler. 2018. Interactive effects of acidification, hypoxia, and thermal stress on growth, respiration, and survival of four North Atlantic bivalves. Marine Ecology Progress Series. **604:** 143 – 161. doi: 10.3354/meps12725

Stokesbury, K. D. E., B. P. Harris, M. C. Marino II, and J. I. Nogueira. 2004. Estimation of sea scallop abundance using a video survey in off-shore US waters. Journal of Shellfish Research. **23(1):** 33 – 40.

Sutton, J. N., Y.-W. Liu, J. B. Ries, M. Guillermic, E. Ponzevera, and R. A. Eagle. 2018. $\delta^{11}B$ as monitor of calcification site pH in divergent marine calcifying organisms. Biogeosciences. **15:** 1447 – 1467. doi: 10.5194/bg-15-1447-2018

Talmage, S. C. and C. J. Gobler. 2011. Effects of Elevated Temperature and Carbon Dioxide on the Growth and Survival of Larvae and Juveniles of Three Species of Northwest Atlantic Bivalves. PloS One. **6(10):** e26941. doi: 10.1371/journal.pone.0026941

887 Thomsen, J., K. Haynert, K. M. Wegner, and F. Melzner. 2015. Impact of seawater carbonate
888 chemistry on the calcification of marine bivalves. Biogeosciences. **12:** 4209 – 4220. doi:
889 10.5194/bg-12-4209-2015
890
891 Toyofuku, T., M. Y. Matsuo, L. J. de Nooijer, Y. Nagai, S. Kawada, K. Fujita, G.-J. Reichart, H.
892 Nomaki, M. Tsuchiya, H. Sakaguchi, and H. Kitazato. 2017. Proton pumping accompanies
893 calcification in foraminifera. Nature Communications. **8:** 14145. doi: 10.1038/ncomms14145
894
895 Waldbusser, G. G., H. Bergschneider, and M. A. Green. 2010. Size-dependent pH effect on
896 calcification of post-larval hard clam *Mercenaria* spp. Marine Ecology Progress Series. **417:** 171
897 – 182. doi: 10.3354/meps08809
898
899 Waldbusser, G. G., B. Hales, C. J. Langdon, B. A. Haley, P. Schrader, E. L. Brunner, M. W.
900 Gray, C. A. Miller, and I. Gimenez. 2015. Saturation-state sensitivity of marine bivalve larvae to
901 ocean acidification. Nature Climate Change. **5:** 273 – 280. doi:
902
903 White, M. M., D. C. McCorkle, L. S. Mullineaux, and A. L. Cohen. 2013. Early Exposure of Bay
904 Scallops (*Argopecten irradians*) to High CO_2 Causes a Decrease in Larval Shell Growth. PloS
905 One. **8(4):** e61065. doi: 10.1371/journal.pone.0061065
906
907 Wilbur, K. M. and A. M. Bernhardt. 1983. Effects of amino acids, magnesium, and molluscan
908 extrapallial fluid on crystallization of calcium carbonate: *in vitro* experiments. The Biological
909 Bulletin. **166(1):** 251 – 259. doi: 10.2307/1541446

Wood, H. L., J. I. Spicer, and S. Widdicombe. 2008. Ocean acidification may increase calcification rates, but at a cost. Proceedings of the Royal Society B: Biological Sciences. **275(1644):** 1767 – 1773. doi: 10.1098/rspb.2008.0343

Xie, J., J. Liang, J. Sun, J. Gao, S. Zhang, Y. Liu, L. Xie, and R. Zhang. 2016. Influence of the extrapallial fluid of *Pinctada fucata* on the crystallization of calcium carbonate and shell biomineralization. Crystal Growth and Design. **16(2):** 672 – 680. doi: 10.1021/acs.cgd.5b01203

Zhao, X., W. Shi, Y. Han, S. Liu, C. Guo, W. Fu, X. Chai, and G. Liu. 2017. Ocean acidification adversely influences metabolism, extracellular pH and calcification of an economically important marine bivalve *Tegillarca* granosa. Marine Environmental Research. **125:** 82 – 89. doi: 10.1016/j.marenvres.2017.01.007

Zhao, L., F. Yang, S. Milano, T. Han, E. O. Walliser, and B. R. Schöne. 2018. Transgenerational acclimation to seawater acidification in the manila clam *Ruditapes philippinarum:* preferential uptake of metabolic carbon. Sci. Tot. Env. **627:** 95 – 103. doi: 10.1016/j-scitotenv/2018.01.225

Zoccola, D., E. Tambutté, E. Kulhanek, S. Puverel, J.-C. Scimeca, D. Allemand, D. and S. Tambutté. 2004. Molecular cloning and localization of a PMCA P-type calcium ATPase from the coral *Stylophora pistillata.* Biochimica et Biophysica Acta (BBA) – Biomembranes. **1663:** 117 – 126. doi: 10.1016/j.bbamem.2004.02.010

Acknowledgements

This research was funded by NOAA award NA14NMF4540072 to JBR and JHG, NOAA/MIT SeaGrant awards NA14OAR41705710004054 and NA18OAR4170105 to JBR, and NSF-BIO-OCE award #1437371 to JBR. We thank Nordic Inc and the crew of the FV Liberty, I. Westfield, and N. Krlovic for assistance in the field. We also thank I. Westfield for advice on setting up the tank experiment, J. Gunnell for advice on statistical analysis, J. Salisbury for access to the Apollo Scitech DIC Analyzer at the University of New Hampshire, and C. Hunt for training on this instrument.

Statement of Author Contributions

The experiment was conceived of and designed by JBR and JHG and refined with input from LPC. The experiment was conducted by LPC. Data were analyzed and interpreted by LPC with assistance from JBR and JHG. Statistical tests and data visualization were performed by LPC. The manuscript was written by LPC with assistance from JBR and JHG. All authors contributed to editing the manuscript and have approved of its final submission.

Conflict of interest statement

All authors declare that they have no conflict of interest.